Recombinant two-iron rubredoxin of *Pseudomonas oleovorans*: overexpression, purification and characterization by optical, CD and ^{113}Cd NMR spectroscopies

Ho Joon LEE*, Lu-Yun LIAN†[1] and Nigel S. SCRUTTON*[1]

*Department of Biochemistry, University of Leicester, Adrian Building, University Road, Leicester LE1 7RH, U.K., and †Biological NMR Centre, University of Leicester, Medical Sciences Building, University Road, Leicester LE1 9HN, U.K.

The gene (*alk* G) encoding the two-iron rubredoxin of *Pseudomonas oleovorans* was amplified from genomic DNA by PCR and subcloned into the expression vector pKK223-3. The vector directed the high-level production of rubredoxin in *Escherichia coli*. A simple three-step procedure was used to purify recombinant rubredoxin in the 1Fe form. 1Fe-rubredoxin was readily converted to the 2Fe, apoprotein and cadmium forms after precipitation with trichloroacetic acid and resolubilization in the presence or absence of ferrous ammonium sulphate or $CdCl_2$ respectively. Recombinant 1Fe and 2Fe rubredoxins are redox-active and able to transfer electrons from reduced spinach ferredoxin reductase to cytochrome *c*. The absorption spectrum and dichroic features of the CD spectrum for the cadmium-substituted protein are similar to those reported for cadmium-substituted *Desulfovibrio gigas* rubredoxin [Henehan, Poutney, Zerbe and Vasak (1993) Protein Sci. **2**, 1756–1764]. Difference absorption spectroscopy of cadmium-substituted rubredoxin revealed the presence of four Gaussian-resolved maxima at 207, 228, 241 and 280 nm; the 241 nm band is attributable, from Jørgensen's electronegativity theory, to a $CysS–Cd^{II}$ charge-transfer excitation. The ^{113}Cd NMR spectrum of the ^{113}Cd-substituted rubredoxin contains two ^{113}Cd resonances with chemical shifts located at 732.3 and 730 p.p.m. The broader linewidth and high frequency shift of the resonance at 730 p.p.m. indicates that the Cd^{2+} ion is undergoing chemical exchange and, consistent with the difference absorption spectra, is bound less tightly than the Cd^{2+} ion, giving rise to the chemical shift at 732.3 p.p.m.

INTRODUCTION

The rubredoxins are non-haem iron proteins whose active sites comprise an iron atom tetrahedrally co-ordinated to four cysteine residues [1]. Rubredoxins serve as electron carriers and most have a molecular mass of approx. 6 kDa. Most rubredoxins are restricted to anaerobes, and NADH-dependent rubredoxin reductases have been partly purified from some of these organisms [2–4]. Although rubredoxins are presumed to function as electron carriers, the rubredoxin of *Pseudomonas oleovorans* is the only member of this family of proteins for which the electron transfer reactions have been delineated in detail. In this organism, rubredoxin is one of three components required for alkane hydroxylation [5]. The recent cloning and sequencing of the genes encoding proteins involved in the hydroxylation of alkanes [6,7] has established the role of rubredoxin in transferring electrons from a specific rubredoxin reductase to the 'ω-hydroxylase', a membrane-bound di-iron-protein responsible for the hydroxylation of alkane substrates. The *Ps. oleovorans* rubredoxin is unique in that it contains two binding sites for iron. Unlike other rubredoxins (molecular mass approx. 6 kDa), the *Ps. oleovorans* rubredoxin is a 19 kDa protein and the gene encoding the protein (*alk* G) [6] is most probably the product of a gene duplication event. The 2Fe form of the rubredoxin is believed to be the physiological form, but it is less stable than the readily isolated 1Fe form [8]. This latter form of the rubredoxin is also active in its reaction with rubredoxin reductase [8].

Rubredoxins have been studied extensively from the structural viewpoint. Three-dimensional structures with resolutions better than 1.5 Å have been reported [9–14] and NMR studies have been utilized to investigate metal ion ligation [15,16], contributions made by protein structure to the overall thermostability of rubredoxins [17] and solution structure [18]. However, despite this detailed structural knowledge, little is known about the function of rubredoxins in general. With this deficiency in mind, we have chosen to study the rubredoxin from *Ps. oleovorans* for which there is a well-defined biochemical role, namely the transfer of electrons from rubredoxin reductase to the membrane-bound ω-hydroxylase during the hydroxylation of alkanes. A structural determination of the 2Fe rubredoxin, rubredoxin reductase and ultimately the productive electron transfer complex formed by the two proteins will provide valuable information on electron transfer mechanisms in this physiological redox system. With this ultimate goal in mind, we describe here the production of recombinant 2Fe rubredoxin and the generation of Cd-substituted forms that are suitable for studies with NMR spectroscopy. Rubredoxin was the first non-haem iron protein studied by ^1H NMR spectroscopy; in the oxidized form, the long correlation time of the Fe^{3+} ion causes large broadening of the β-CH_2 cysteine proton signals so that they are undetectable [19,20]. To overcome the problems caused by the paramagnetism of the iron centre, the NMR-active isotope of cadmium, ^{113}Cd, has often been used to probe the environment around the metal ligand. In the present study we replaced the native Fe^{3+} ion with the $^{113}Cd^{2+}$ ion and investigated the NMR and optical properties of the Cd-substituted protein. One-dimensional (1D) and two-

Abbreviations used: 1D, 2D, one-dimensional, two-dimensional; HSQC, heteronuclear single-quantum correlation.

[1] To whom correspondence should be addressed.

dimensional (2D) NMR experiments were performed to identify the ^{113}Cd–cysteine connectivities for the large $^{3}J(^{1}H^{\beta}–^{113}Cd)$ values. The longer overall correlation time of *Ps. oleovorans* rubredoxin (19 kDa), compared with other smaller ^{113}Cd-substituted rubredoxins that have been studied in a similar manner, makes detection of the $^{1}H^{\beta}–^{113}Cd$ connectivities with very small coupling constant difficult.

MATERIALS AND METHODS

Materials

Complex bacteriological media were from Unipath and all media were prepared as described by Sambrook et al. [21]. Ethidium bromide, isopropyl β-D-thiogalactoside, horse cytochrome *c*, spinach ferredoxin reductase, $CdCl_2$ and ferrous ammonium sulphate were from Sigma.

$^{113}CdCl_2$ was from Promochem. Vent DNA polymerase was from New England Biolabs. Restriction enzymes *Sma*I, *Eco*RI, Phenyl-Sepharose and the expression vector pKK223-3 were from Pharmacia. Calf intestinal alkaline phosphatase was supplied by Boehringer. Timentin was from Beecham Research Laboratories. Wizard PCR purification kits were from Promega. DE-52 anion-exchange resin was from Whatman. All other chemicals were of A.R. grade wherever possible. Glass-distilled water was used throughout. *Ps. oleovorans* strain GPO1 was a gift from Professor B. Witholt (Institute of Biotechnology, ETH, Zurich, Switzerland) and was maintained on solid medium with hexane vapour as sole carbon source.

Recombinant DNA methods

Bacteria were cultured in double-strength YT medium supplemented, where appropriate, with Timentin. Plasmid DNA was prepared by CsCl density centrifugation, and general cloning methods were adopted from Sambrook et al. [21]. *Ps. oleovorans* chromosomal DNA for PCR was prepared by suspending a single colony from a plate in 0.5 ml of water. The suspension was boiled for 5 min and centrifuged for 2 min to remove debris. Supernatant (5 μl) was used as template for PCR reactions. The *alk* G gene encoding rubredoxin was amplified from chromosomal DNA with the oligonucleotides 5′-TTTTTTTTTGAATTCATGGCTAGCTATAAATGCCCGGAT-3′ and 5′-TTTTTTTTTCCCGGGTCACTTTTCCTCGTAGAGCACATA-3′. Primers were synthesized in accordance with the published DNA sequence [6] and were designed so as to incorporate a unique *Eco*RI site (N-terminal oligonucleotide) or *Sma*I site (C-terminal oligonucleotide) to allow directional ligation of the amplified product into plasmid pKK223-3 after digestion with *Eco*RI and *Sma*I. The recombinant plasmid, designated pKR10, was maintained in *E. coli* strain TG1. The entire *alk* G gene was resequenced by the dideoxy chain termination method [22] by automated fluorescent sequencing with a Pharmacia LKB ALF sequencer to ensure that mutations did not arise during the amplification process.

Protein expression and purification

For the large-scale purification of rubredoxin, *E. coli* strain TG1 transformed with pKR10 was grown in 10 litres of 2 × YT medium supplemented with 50 μg/ml timentin. Cells were harvested in early stationary phase, washed with 0.1 M potassium phosphate buffer, pH 7.5 (buffer A), and collected again by centrifugation. The cells were then suspended in 150 ml of buffer A and disrupted in a French press at 4 °C at a pressure of 140 MPa. The extract was clarified by centrifugation at 15000 ***g*** for 90 min and fractionated with solid $(NH_4)_2SO_4$.

During additions of $(NH_4)_2SO_4$, the cell-free extract developed an intense red–brown colour, indicating oxidation of the reduced rubredoxin. The precipitate with 40–60 %-satd. $(NH_4)_2SO_4$, which contained the rubredoxin, was dissolved in approx. 100 ml of buffer A and dialysed against two changes of buffer A (5 litres each). The dialysed enzyme was then applied to a column (2.5 cm × 10 cm) of DE-52 equilibrated with buffer A. After being washed, the column was developed with a gradient of KCl (0–0.5 M, in buffer A); rubredoxin was found to be eluted at approx. 0.2 M KCl. Fractions containing rubredoxin were pooled and brought to 35 % saturation with $(NH_4)_2SO_4$. The protein was then applied to a phenyl-Sepharose column (2.5 cm × 6 cm) equilibrated with buffer A containing 35 %-satd. $(NH_4)_2SO_4$. The column was developed with a descending gradient of $(NH_4)_2SO_4$ (35–0 % saturation, in buffer A), and rubredoxin was found to be eluted at approx. 20 %-satd. $(NH_4)_2SO_4$. Fractions containing rubredoxin were pooled and concentrated by ultrafiltration. Purified protein was dialysed exhaustively against 50 mM potassium phosphate buffer, pH 7, before storage at −20 °C. The total yield of rubredoxin was approx. 300 mg from a 10 litre cell culture.

CD and NMR spectroscopy

CD spectroscopy was performed with a Jobin Yvon CD6 (Division d-Instruments) instrument with a 0.5 mm path length. Six scans, over the range 195–260 nm at 20 °C, were averaged. Integration time was 3 s per nm scanned. No smoothing algorithms were employed. Sample concentration was 1 mg/ml for all samples.

The ^{1}H and ^{113}Cd NMR spectra were recorded with a Bruker AMX-600 spectrometer. The NMR sample (0.5–1.0 mM protein in 20 mM potassium phosphate buffer, pH 7.6) was made up in either 90 % H_2O/10 % $^{2}H_2O$ or 99 % $^{2}H_2O$. Spectra were recorded at 298 and 313 K. The chemical shifts of ^{113}Cd were referenced to 0.1 M $^{113}Cd(ClO_4)_2$ at 0 p.p.m. Proton chemical shifts were referenced to the water resonance at 4.80 p.p.m. Homonuclear 2D double-quantum-filtered COSY, TOCSY and NOESY data were acquired with standard pulse sequences; where appropriate, ^{113}Cd-decoupling, with a globally optimized alternating-phase rectangular-pulses decoupling sequence, was incorporated during the evolution and acquisition periods. For all experiments, solvent suppression was achieved by a low-power pre-irradiation. To obtain $^{113}Cd–^{1}H$ connectivities, a standard heteronuclear single-quantum correlation (HSQC) pulse sequence was used with polarization transfer delays optimized for coupling constants of either 40 or 17 Hz. All heteronuclear experiments were performed with ^{113}Cd-decoupling during acquisition. All spectra were measured in phase-sensitive modes. COSY data matrices were 4096 × 512; NOESY data matrices were 2048 × 512 and $^{113}Cd–^{1}H$ 2D HSQC matrices were 4096 × 128 real-time domain data points.

Redox potentiometry and kinetic measurements

Potentiometric titrations of the 1Fe and 2Fe forms of rubredoxin were conducted with the xanthine oxidase method developed by Massey [23]. Rubredoxin was contained in 100 mM potassium phosphate buffer, pH 7.0. Rubredoxin was made anaerobic in a side-arm cuvette along with 290 μM xanthine, 2 μM Methyl Viologen and 50 μM Indigo Tetrasulphonate (−46 mV) in a total volume of 2 ml. Xanthine oxidase (5 μl of a 66 μM stock) was placed in the side arm of the apparatus. After achievement of anaerobosis by repeated evacuation and flushing with O_2-free argon, the UV–visible spectrum of the mixture was recorded with a Hewlett Packard 8452a diode-array spectrophotometer. Re-

duction of the dye was initiated by tipping xanthine oxidase from the side arm into the mixture. Spectra were recorded at 5 min intervals. The extent of reduction of rubredoxin and the dye were determined from absorbance changes at 484 nm and 588 nm respectively. The mid-point potential of rubredoxin was determined from a plot of log[Indigo Tetrasulphonate$_{ox}$]/[Indigo Tetrasulphonate$_{red}$] against log[rubredoxin$_{ox}$]/[rubredoxin$_{red}$].

Steady-state kinetic measurements were performed with a 1 cm light path in a final volume of 1 ml. The desired concentrations of horse heart cytochrome *c* (81 μM), rubredoxin (0–80 nM), spinach ferredoxin reductase (500 nM) and NADPH (300 μM) were obtained by making microlitre additions from stock solutions to the assay mixture. Assays were performed in 50 mM Tris/HCl buffer, pH 7.8, containing 15 μM BSA. Reactions were started by the addition of NADPH; the increase in absorption at 550 nm due to the reduction of cytochrome *c* (ϵ_{550} 21 000 $M^{-1} \cdot cm^{-1}$) was measured with a Hewlett Packard 8452a single-beam diode-array spectrophotometer. All data were collected at 30 °C.

RESULTS AND DISCUSSION

Overexpression and purification of *Ps. oleovorans* rubredoxin in *E. coli*

The gene (*alk* G) encoding the rubredoxin of *Ps. oleovorans* was amplified from genomic DNA by PCR. After amplification the product was digested with *Eco*RI/*Sma*I and ligated directionally into plasmid pKK223-3, which had previously been digested with the same enzymes. In the resultant plasmid (pKR10), the *alk* G gene comes under the control of the *tac* promoter. Transformation of *E. coli* strain TG1 with plasmid pKR10 leads to the high-level expression of rubredoxin (Figure 1). The inclusion of isopropyl β-D-thiogalactoside (2 mM) in cultures of TG1 transformed with pKR10 did not lead to further increases in the level of expression of rubredoxin.

Recombinant rubredoxin was purified as described above; an analysis of rubredoxin purity by SDS/PAGE at various stages of the purification is shown in Figure 2. Samples for electrophoresis were produced from freshly prepared material and stored in SDS electrophoresis sample buffer until required. Rubredoxin samples subjected to electrophoresis immediately after preparation in the presence of sample buffer containing 50 mM dithiothreitol migrated as a single band; however, samples prepared in the absence of dithiothreitol migrated as multiple bands, indicating the ease with which disulphide links are formed with this protein (Figure 2).

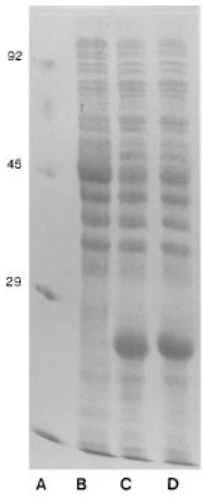

Figure 1 Expression of *Ps. oleovorans* rubredoxin in *E. coli* strain TG1

Samples of cell extracts were prepared and analysed by means of SDS/PAGE. Protein bands were stained with Coomassie Brilliant Blue. Lane A, molecular mass markers (molecular masses in kDa are indicated at the left); lane B, untransformed *E. coli* strain TG1; lane C, *E. coli* strain TG1 transformed with plasmid pKR10; lane D, *E. coli* strain TG1 transformed with plasmid pKR10 induced with 2 mM isopropyl β-D-thiogalactoside.

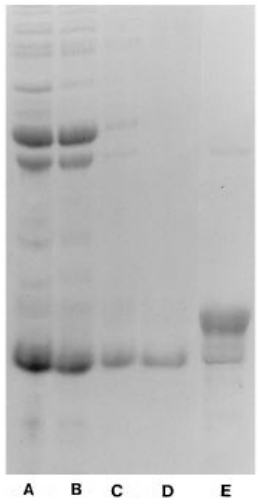

Figure 2 Purification of *Ps. oleovorans* rubredoxin from *E. coli* strain TG1 transformed with plasmid pKR10

Samples of protein at various stages in the purification were analysed by means of SDS/PAGE. Protein bands were stained with Coomassie Brilliant Blue. Lane A, cell free extract; lane B, $(NH_4)_2SO_4$ fraction; lane C, pooled fractions after ion-exchange chromatography; lane D, pooled fractions after hydrophobic interaction chromatography; lane E, as lane D but without dithiothreitol in sample buffer.

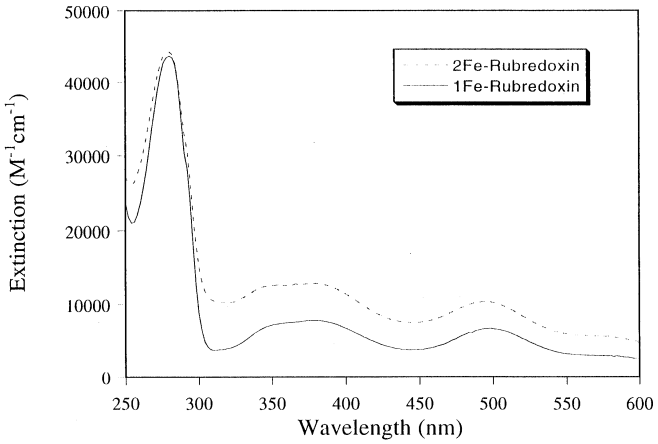

Figure 3 UV–visible spectra of 1Fe and 2Fe forms of rubredoxin

Spectra were recorded of protein samples in 50 mM potassium phosphate buffer, pH 7.0.

Spectral, redox and kinetic properties of recombinant rubredoxins

The absorption spectrum of the purified protein has absorption maxima at 498, 380 and 280 nm, with an A_{280}-to-A_{498} ratio of 6.4:1 (Figure 3). The A_{280}-to-A_{498} ratio is similar to that reported

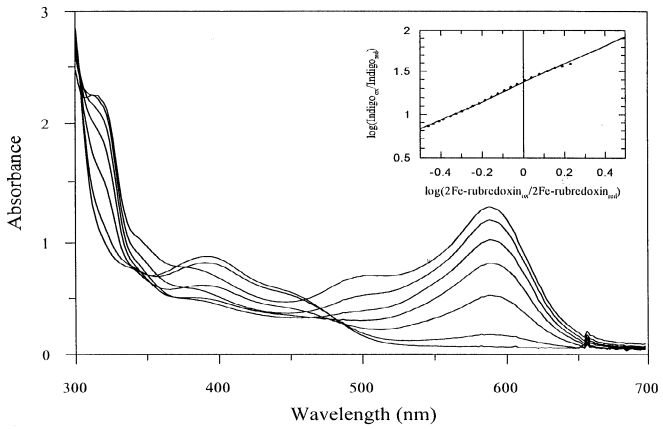

Figure 4 Midpoint potential determination of the 2Fe form of rubredoxin

Oxidized rubredoxin in 100 mM potassium phosphate buffer, pH 7.0, was mixed with 50 μM Indigo Tetrasulphonate, 2 μM Methyl Viologen, 290 mM xanthine and 165 nM xanthine oxidase under anaerobic conditions. Scans were recorded every 5 min (not all results are shown). Inset: plot of log[Indigo Tetrasulphonate$_{ox}$]/[Indigo Tetrasulphonate$_{red}$] against log[rubredoxin$_{ox}$]/[rubredoxin$_{red}$]. Midpoint potential is -6 mV. A similar plot for 1Fe rubredoxin yielded a midpoint potential of -8 mV.

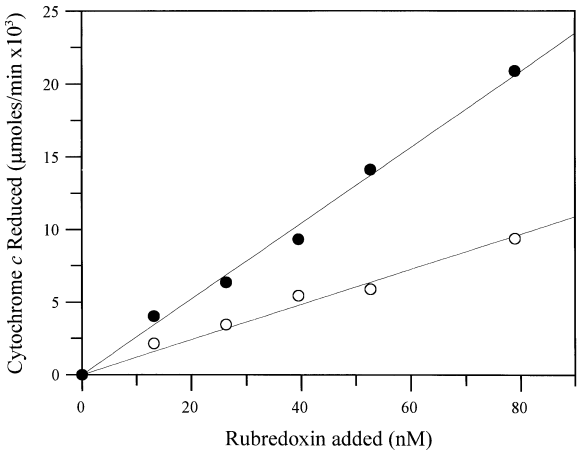

Figure 5 Reduction of cytochrome *c* by 1Fe and 2Fe forms of recombinant rubredoxin and spinach ferredoxin reductase

Linear fits indicate that the gradient for the 2Fe rubredoxin is twice that for 1Fe rubredoxin. Symbols: ●, 2Fe rubredoxin; ○, 1Fe rubredoxin.

previously for the purification of *Ps. oleovorans* rubredoxin from a native source, which was shown to correspond to 1Fe rubredoxin [8]. Recombinant 1Fe rubredoxin was readily converted to the 2Fe form by methods evolved from the reconstitution of rubredoxins from anaerobic bacteria (see, for example, [8]). Protein was precipitated at room temperature with trichloroacetic acid [10% (w/v) final concentration] and harvested by centrifugation. Subsequent steps were performed under an argon atmosphere. The precipitated apoprotein was dissolved at a final concentration of approx. 5 mg/ml in 0.5 M Tris base containing 0.5 M 2-mercaptoethanol, and argon was bubbled through the solution for 10 min. The protein was then incubated at room temperature for 3 h and re-precipitated with trichloroacetic acid. The precipitate was resolubilized in 0.5 M Tris base and a 5-fold molar excess of ferrous ammonium sulphate was added. After a

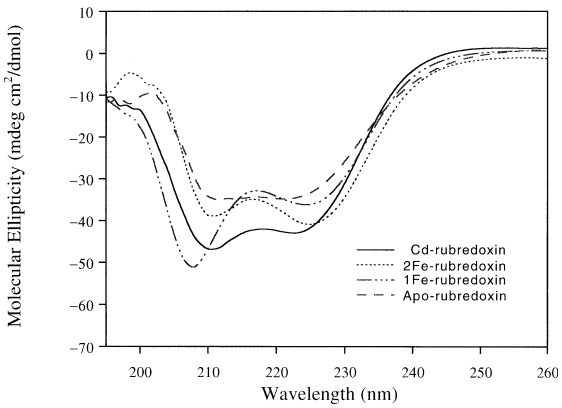

Figure 6 Far-UV CD spectra of the various forms of *Ps. oleovorans* rubredoxin

Spectra were recorded of samples in 50 mM potassium phosphate buffer, pH 7.0.

10 min incubation on ice, air was admitted and the solution turned dark red. Rubredoxin was then desalted with a small Sephadex G25 column equilibrated with 50 mM potassium phosphate buffer, pH 7.5, to remove ferrous ammonium sulphate. The absorption spectrum of the reconstituted protein had absorption maxima at 496, 378 and 280 nm and an A_{280}-to-A_{496} ratio of 4.1:1, indicating that the reconstituted protein was present in the 2Fe form [8] (Figure 3).

The midpoint potentials of the recombinant 1Fe (-8 mV) and 2Fe (-6 mV) rubredoxins were found to be similar (Figure 4), indicating that the presence or absence of iron at one binding site has little or no influence on the reduction potential of the iron bound at the second site. Steady-state assays of cytochrome reduction by 1Fe and 2Fe rubredoxin indicated that the 2Fe form is about twice as active as the 1Fe form (Figure 5). The results suggest that both domains are active in transferring electrons from spinach ferredoxin reductase to cytochrome *c*.

Preparation and characterization of cadmium-substituted rubredoxin

Cadmium-substituted rubredoxin was isolated with an adaptation of the method developed for the preparation of 2Fe rubredoxin described above. For Cd substitution, a 5-fold molar excess of $CdCl_2$ over protein replaced ferrous ammonium sulphate in the reconstitution method. All other steps were as described for the production of 2Fe rubredoxin. To investigate the effects on protein secondary structure of replacing iron with cadmium, the far-UV spectra of 1Fe, 2Fe, apo- and cadmium-substituted rubredoxins were recorded between 260 and 195 nm (Figure 6). The CD spectrum of the 2Fe rubredoxin has two negative bands at 210 and 225 nm. The spectrum of aporubredoxin is similar in form to that of 2Fe rubredoxin, indicating that the overall protein structure is essentially retained on removal of the metal ions. The spectrum of 1Fe rubredoxin indicates that structural changes do occur on removal of one iron from the protein. The larger negative band below 210 nm probably reflects a less ordered conformation in the 1Fe rubredoxin, and this is consistent with a small increase in the CD signal at approx. 218 nm. Metal-dependent changes are seen in the CD spectrum of cadmium-substituted rubredoxin above 200 nm, and the trends are similar to those seen for cadmium-substituted *Desulfovibrio gigas* rubredoxin [15]. In the latter case, cadmium-substituted

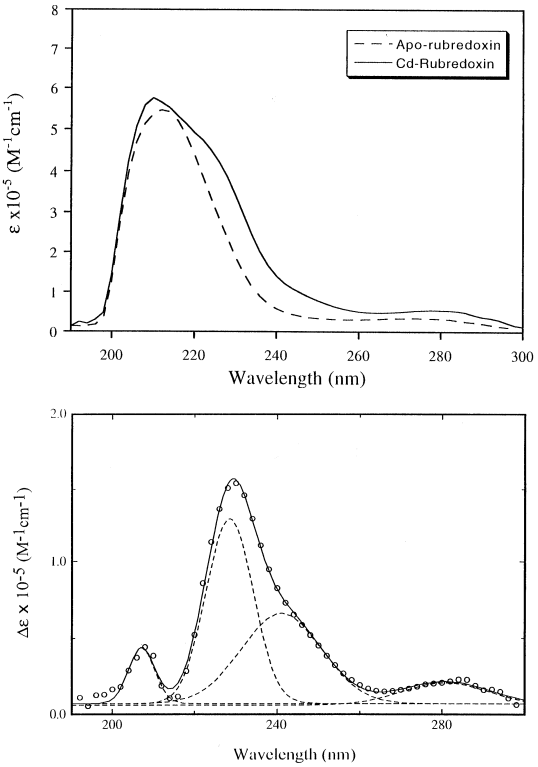

Figure 7 Optical spectra and difference spectra for Cd-substituted *Ps. oleovorans* rubredoxin

Upper panel: optical spectra for Cd-substituted rubredoxin and aporubredoxin. Lower panel: difference optical spectra and the results of the Gaussian analysis of the difference absorption spectra. Broken lines, individual component bands; solid line, sum of the Gaussian components; ○, difference spectrum.

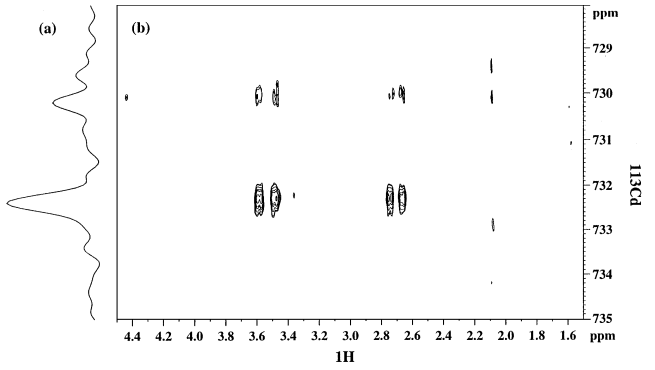

Figure 8 NMR spectra of Cd-substituted *Ps. oleovorans* rubredoxin

1D ^{113}Cd spectrum (**a**) and 2D [^{113}Cd–^{1}H] HSQC spectrum (**b**) of *Ps. oleovorans* rubredoxin recorded at 40 °C and pH 7.6. The 2D spectrum was acquired with a polarization transfer delay of 6 ms.

rubredoxin is thought to be isostructural with native *D. gigas* rubredoxin. Similarly, we expect that cadmium substitution of *Ps. oleovorans* rubredoxin is also isostructural with the native 2Fe form.

The electronic absorption spectrum of cadmium-substituted rubredoxin revealed the presence of a broad absorption between 200 and 300 nm superimposed on the spectrum of the apoprotein (Figure 7); the difference absorption spectrum can be resolved into four Gaussian bands located at 207, 228, 241 and 280 nm. The increase in absorption at 280 nm for the cadmium-substituted protein compared with apoprotein most probably reflects a sharpening of tryptophan absorption by the metal ion. Similar effects have been seen in *D. gigas* rubredoxin, in which the metal ion is known to be located near the indole ring of a single tryptophan residue [15]. *Ps. oleovorans* rubredoxin contains four tryptophan residues and two of these are adjacent in sequence to a cysteinyl ligand in each of the metal-binding sites. The electronegativity concept of Jørgensen [24] attributes the lowest energy absorption of the remaining three bands (241 nm) to a Cd–thiolate charge-transfer transition. By using the previously determined absorption coefficient for this transition in *D. gigas* cadmium-substituted rubredoxin (6500 $M^{-1} \cdot cm^{-1}$) [15], we calculate the presence of approx. 8.9 Cys-Cd bonds in the *Ps. oleovorans* cadmium-substituted protein. Because the two metal-binding sites can contribute only eight Cys-Cd bonds when fully occupied, the results suggest an absorption coefficient of approx. 7200 $M^{-1} \cdot cm^{-1}$ for *Ps. oleovorans* Cd-substituted rubredoxin. In practice, the absorption coefficient for Cys-Cd bonds in a variety of proteins is variable (see, for example, [15]) and fall within a range of values; although 7200 $M^{-1} \cdot cm^{-1}$ might be at the higher end of this range, it is not unacceptably high. Because only two ^{113}Cd signals are seen for cadmium-substituted rubredoxin (see below), it is clear that the additional two Cys residues that do not form the iron-binding site are also not ligands for Cd. These latter two Cys residues therefore do not contribute to absorption changes at 241 nm. The precise assignment of the remaining two bands (207 and 228 nm) in the optical difference spectrum remains to be determined but, as in *D. gigas* rubredoxin, it is clear that they are predominantly charge-transfer in character [15].

NMR spectroscopy of the ^{113}Cd-substituted protein

Comparison of the chemical shifts in the homonuclear 2D ^{1}H spectra of the 2Cd *Ps. oleovorans* rubredoxin with published spectra of the zinc-containing *Clostridium pasteurianum* rubredoxin [17] suggests that the protein has two folded domains and a long flexible region. This is expected from sequence alignment predictions. Although the linewidths of the resonances are narrow for a 19 kDa protein, the TOCSY spectra suggest that the overall correlation time of the protein is shorter than that for a single rubredoxin domain of molecular mass 6 kDa. Whether there is an interaction between the two domains or whether these are entirely independent remains to be determined when sequence-specific assignment of the spectra and detailed analysis of the interproton NOEs and relaxation times have been completed. The 1D ^{113}Cd spectrum shows two resonances at 732.3 and 730 p.p.m., although the two resonances do not have the same intensities and linewidths: the resonance at 732.3 p.p.m. is sharper than the resonance at 730 p.p.m. (Figure 8a). The chemical shift positions of these resonances correspond well with other tetrahedral tetrathiolate cadmium sites (610–750 p.p.m.) [25]. The result implies that there are two Cd^{2+} ions present in the protein and that they are not identical in their NMR characteristics. The broader linewidth and large frequency shift of the resonance at 730 p.p.m. indicate that the Cd^{2+} ion is undergoing some chemical exchange and hence is possibly bound less strongly than the other Cd^{2+} ion. These spectra demonstrate one of the

main benefits that can be obtained from the very good resolution of ^{113}Cd spectra; even when ^{113}Cd ion binds to different co-ordination sites of very similar structure, as in the present two rubredoxin domains of *Ps. oleovorans*, signals from these two separate sites can be resolved. This capability of detecting and monitoring separate resonances from each metal environment means that it is possible to investigate directly the properties of the two binding sites at the same time. The sensitivity of the chemical shift and linewidth of ^{113}Cd resonances to exchange effects (metal ligand, solvent or substrate exchange) makes ^{113}Cd NMR a good probe for studying the catalytic and binding mechanisms. More detailed investigation of these ^{113}Cd signals from *Ps. oleovorans* rubredoxin is currently in progress.

The positions of β proton chemical shifts of the cysteine residues that are liganded to the Cd^{2+} ions are identified from the 2D (^{1}H–^{113}Cd) HSQC experiments (Figure 8b). To optimize the polarization transfer, delay times of between 6 and 25 ms were tried by using the 1D (^{1}H–^{113}Cd) HSQC pulse sequence. Owing to the shorter transverse relaxation time of the larger *Ps. oleovorans* rubredoxin protein than for other Cd-substituted proteins previously studied with ^{1}H–^{113}Cd heteronuclear NMR methods [15,26,27], it is only possible to detect the ^{1}H signals when the $^3J(^1H^{\beta}–^{113}Cd)$ coupling constant is greater than 15 Hz; experiments performed with delays optimized for smaller coupling constants led to significant losses in signal to noise. From the present 2D (^{1}H–^{113}Cd) HSQC data, the chemical shifts of eight sets of cysteine β protons were identified, four from the two cysteine residues liganded to the Cd^{2+} ion at 732.3 p.p.m. and the other four to the Cd^{2+} ion at 730 p.p.m. (Figure 8b). It is interesting to note that the β chemical shifts of the cysteine residues separately liganded to the two Cd^{2+} ions are degenerate, i.e. there are only four different cysteine β proton chemical shifts. Combining the 2D (^{1}H–^{113}Cd) HSQC, and the double-quantum COSY spectra with and without ^{113}Cd decoupling, it is possible to delineate the chemical shifts of the two sets of cysteine residues where $^3J(^1H^{\beta}–^{113}Cd)$ is larger than 15 Hz: 5.530, 3.632, 2.714 p.p.m. and 5.226, 3.535, 2.788 p.p.m. for H^{α}, $H^{\beta\alpha}$, $H^{\beta\beta}$ respectively. The weakness of the resonances from the cysteine residue bound to the second cadmium site and the degeneracy of the β resonances, make it difficult to identify the chemical shifts of the cysteine residues in this second site with the double-quantum COSY spectra. The chemical shifts of the cysteine protons identified here correspond well to the reported chemical shifts of zinc-containing *Cl. pasteurianum* rubredoxin [17] and the Cd-substituted *D. gigas* rubredoxin [27]. By deduction we can conclude that there are two groups of $^3J(^1H^{\beta}–^{113}Cd)$ values; one larger than 15 Hz and the other smaller. This is entirely consistent with the $^3J(^1H^{\beta}–^{113}Cd)$ values obtained for *D. gigas* rubredoxin, with the large coupling values representing a *gauche* conformation (defined by the dihedral angle $H^{\beta a,b}–C^{\beta}–S^{\gamma}–Fe$) and the smaller values the *anti* conformation. Assuming that the conformation of the cadmium-substituted protein is identical with that of the native Fe protein [15] it seems that the conformation around the Fe centres for each of the *Ps. oleovorans* rubredoxin domains is similar to that reported for *D. gigas* rubredoxin. Perhaps the main difference between the two *Ps. oleovorans* rubredoxin domains lies in the strength of binding of the metal ion. The isolation of cadmium-substituted *Ps. oleovorans* rubredoxin should now enable the determination of the solution structure of the protein by conventional NMR methods without the added complication of paramagnetic effects imposed by iron.

Received 16 May 1997/2 July 1997; accepted 25 July 1997

This work was supported by the Royal Society University Research Fellowship (N.S.S.). The Leicester Biological NMR Centre is supported by the Biotechnology and Biological Sciences Research Council.

REFERENCES

1 Sieker, L. C., Stenkamp, R. E. and LeGall, J. (1994) Methods Enzymol. **243**, 203–216
2 Stadtman, T. C. (1965) in Non-heme Iron Proteins: Role in Energy Conversion, (San Pietro, E., ed.), pp. 439–445, Antioch Press, Yellow Springs, OH
3 LeGall, J. (1968) Ann. Inst. Pasteur **114**, 109–115
4 Ballongue, J., Amine, J., Masion, E., Petitdemange, H. and Gay, R. (1986) Biochemie **68**, 575–580
5 Peterson, J. A., Basu, D. and Coon, M. J. (1965) J. Biol. Chem. **241**, 5162–5164
6 Eggink, G., van Lelyveld, P. H., Arnbery, A., Arfman, N., Witteveen, C. and Witholt, B. (1987) J. Biol. Chem. **262**, 6400–6406
7 Eggink, G., Engel, H., Vriend, G., Terpestra, P. and Witholt, B. (1990) J. Mol. Biol. **212**, 135–142
8 Lode, E. T. and Coon, M. J. (1971) J. Biol. Chem. **246**, 791–802
9 Watenpaugh, K. D., Sieker, L. C., Herriott, J. R. and Jensen, L. H. (1979) Acta Crystallogr. **B29**, 943–956
10 Frey, M., Sieker, L., Payan, F., Haser, R., Bruschi, M., Pep, G. and LeGall, J. (1987) J. Mol. Biol. **197**, 525–541
11 Stenkamp, R. E., Sieker, L. C. and Jensen, L. H. (1990) Proteins: Struct. Funct. Genet. **8**, 352–364
12 Adman, E. T., Sieker, L. C. and Jensen, L. H. (1991) J. Mol. Biol. **217**, 337–352
13 Dauter, Z., Sieker, L. C. and Wilson, K. S. (1992) Acta Crystallogr. **B48**, 42–49
14 Day, M. W., Hsu, B. T., Joshua-Tor, L., Park, J. B., Zhou, Z. H., Adams, M. W. W. and Rees, D. C. (1992) Protein Sci. **1**, 1494–1507
15 Henehan, C. S., Poutney, D. L., Zerbe, O. and Vasak, M. (1993) Protein Sci. **2**, 1756–1764
16 Poutney, D. L., Henehan, C. J. and Vasak, M. (1995) Protein Sci. **4**, 1571–1576
17 Richie, K. A., Teng, Q., Elkin, C. J. and Kurtz, Jr., D. M. (1996) Protein Sci. **5**, 883–894
18 Blake, P. R., Park, J. B., Zhou, Z. H., Hare, D. R., Adams, M. W. W. and Summers, M. F. (1992) Protein Sci. **1**, 1508–1521
19 Krishnamoorthi, R., Markley, J. L., Cusanovich, M. A. and Przysiecki, C. T. (1986) Biochemistry **25**, 50–54
20 Werth, M. T., Kurtz, Jr., D. M., Moura, I. and LeGall, J. (1987) J. Am. Chem. Soc. **109**, 273–275
21 Sambrook, J., Fritsch, E. F. and Maniatis, T. (1989) Molecular Cloning: A Laboratory Manual, 2nd edn., Cold Spring Harbor Laboratory, Cold Spring Harbor, NY
22 Sanger, F. and Coulson, A. R. (1975) J. Mol. Biol. **94**, 441–448
23 Massey, V. (1990) in Flavins and Flavoproteins, (Curti, B., Ronchi, S. and Zanetti, S., eds.), pp. 59–66, Walter de Gruyter, Berlin
24 Jørgensen, C. K. (1970) Prog. Inorg. Chem. **12**, 101–157
25 Summers, M. F. (1988) Coord. Chem. Rev. **86**, 43–134
26 Gardner, K. H. and Coleman, J. E. (1994) J. Biomed. NMR **4**, 761–774
27 Blake, P. R., Lee, B., Summers, M. F., Adams, M. W. W., Park, J.-B., Zhou, Z. H. and Bax, A. (1992) J. Biomed. NMR **2**, 527–533